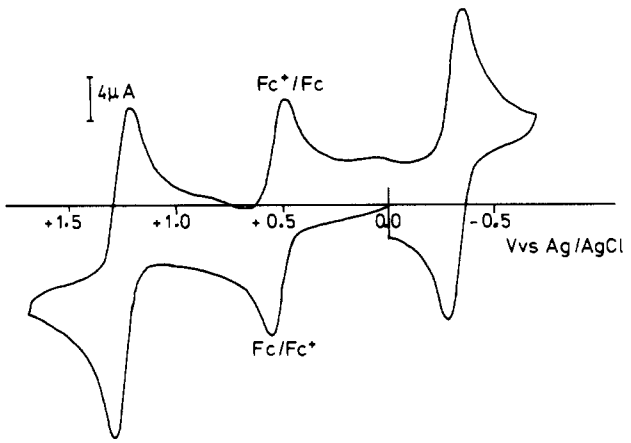

Figure 7. Cyclic voltammogram for $[L_2Ru_2(\mu\text{-}O)_3](PF_6)_2 \cdot H_2O$ in acetonitrile (0.1 M $[TBA]PF_6$) at a scan rate of 100 mV s^{-1} at a platinum-button electrode with ferrocene as internal standard.

This may be interpreted as evidence for the existence of comparatively stronger metal–metal bonding in the μ-hydroxo-bridged species. Upon oxidation of the mixed-valence form, an electron is removed from an antibonding molecular orbital of predominantly metal–metal character.

The CV for $[L_2Ru_2^{IV}(\mu\text{-}O)_3](PF_6)_2$ in acetonitrile is shown in Figure 7. In the potential range −0.7 to +1.7 V vs Ag/AgCl, two reversible one-electron waves are observed at $E^1_{1/2} = +1.12$ V and $E^2_{1/2} = -0.46$ V vs NHE. A coulometric measurement at 1.05 V vs Fc^+/Fc in nitromethane at a glassy-carbon working electrode established that the former corresponds to a one-electron oxidation of the binuclear Ru_2^{IV} species to the $Ru^{IV}Ru^V$ mixed-valence species ($n = 0.99 \pm 0.05$). The dark green color of the solution containing the Ru_2^{IV} complex changed to green-yellow during this oxidation, and the visible absorption spectrum of such an oxidized solution displays maxima at 416, 648, and 1320 nm. The CV recorded on such an oxidized solution was identical with the CV shown in Figure 7. This indicates that on the time scale of a coulometric measurement (≈30 min) the oxidized species is stable. The two one-electron-transfer reactions are thus assigned as in eq 6. Baar and Anson[50] have recently reported on the

$$Ru^{IV}Ru^V \underset{-e^-}{\overset{+e^-}{\rightleftharpoons}} Ru_2^{IV} \underset{-e^-}{\overset{+e^-}{\rightleftharpoons}} Ru^{III}Ru^{IV} \qquad (6)$$
$$E^1_{1/2} \qquad E^2_{1/2}$$

electrochemical behavior of dimeric complexes of $Ru^{III}Ru^{IV}$ and Ru_2^{IV} formed by oxidative dimerization of $[Ru^{III}(edta)OH_2]^-$. The probably oxo-bridged Ru_2^{IV} binuclear complex is capable of oxidizing water.

It is interesting that three μ-oxo bridging groups stabilize the Ru^{IV} oxidation state to such an extent that the $Ru^{IV}Ru^V$ level is readily accessible.

$[L_2Ru_2^{IV}(\mu\text{-}O)_3](PF_6)_2H_2O$ does not react with cyclohexane, ethanol, or benzyl alcohol. This may be due to the fact that the binuclear species is kinetically stable and has no labile coordination sites for substrate binding available.

Acknowledgment. We thank the Fonds der Chemischen Industrie for financial support of this work and the Degussa (Hanau, FRG) for a generous loan of $RuCl_3 \cdot xH_2O$. We are grateful to Professor P. Gütlich (Universität Mainz) for measuring the susceptibility of $[L_2Ru_2(\mu\text{-}O)_3](PF_6)_2 \cdot H_2O$ and Professor A. X. Trautwein (Medizinische Universität Lübeck) for measuring the ESR spectra.

Supplementary Material Available: A list of crystallographic details of the crystal structure determinations (Table S1) and tables of anisotropic displacement factors, H atom coordinates, bond lengths, and bond angles for **1** and **2** (9 pages); listings of observed and calculated structure factors for **1** and **2** (14 pages). Ordering information is given on any current masthead page.

(50) Baar, R. B.; Anson, F. C. *J. Electroanal. Chem. Interfacial Electrochem.* **1985**, *187*, 265.

Contribution from the Departments of Chemistry, Washington University, St. Louis, Missouri 63130, and Louisiana State University, Baton Rouge, Louisiana 70803-1804

Conformational Studies and Reduction Chemistry of a Bimetallic Cobalt(I) Carbonyl Complex Based on a Binucleating Hexakis(tertiary phosphine) Ligand System

Andre D'Avignon,[1a] Fredric R. Askham,[1a] and George G. Stanley*[,1b]

Received January 2, 1990

The 300- and 500-MHz ^1H NMR spectra of the bimetallic complex $Co_2(CO)_4(eHTP)^{2+}$ (eHTP = $(Et_2PCH_2CH_2)_2PCH_2P(CH_2CH_2PEt_2)_2$) show a number of solvent-dependent and, in the case of acetone, temperature-dependent shifts of the central methylene bridge and chelate ring proton resonances. The results of two-dimensional ^1H *J*-correlated experiments, with and without ^{31}P decoupling, are presented to assign both ^1H–^1H and ^1H–^{31}P coupling constants in acetone-d_6 and CD_2Cl_2. Broad-band ^{31}P decoupling causes a spectacular simplification of the highly coupled ^1H spectra, allowing clear resolution of all resonances. van der Waals energy calculations are presented for a model complex of $Co_2(CO)_4(eHTP)^{2+}$ that show the presence of several low-energy conformers differing by rotations about the central methylene bridge. The chemical shift changes for the P–CH_2–P proton resonances are proposed to be caused by differing amounts of carbonyl shielding from different rotational conformers in solution. The changes in the chelate ring proton resonances are proposed to be caused by trigonal-bipyramidal ⇄ square-pyramidal coordination geometry changes about the cobalt centers, which result in chelate ring conformational changes. The reduction of $Co_2(CO)_4(eHTP)^{2+}$ with naphthalenide anion produces the Co–Co-bonded dimer $Co_2(CO)_2(eHTP)$ in 40–50% yields. This very reactive material has been spectroscopically characterized, and both one-dimensional ^{31}P NMR and two-dimensional ^{31}P–^{31}P COSY NMR spectra for the product mixture are presented and discussed.

Introduction

The hexaphosphine ligand system $(Et_2PCH_2CH_2)_2PCH_2P(CH_2CH_2PEt_2)_2$, eHTP, was designed to both bridge and chelate two transition-metal centers, and we have found that this alkylated, electron-rich phosphine is an extremely powerful binucleating ligand system. So far every time we have added 2 equiv of a simple mononuclear metal halide (or related) complex we have obtained a bimetallic species, usually in high yield. Although the ligand was designed to produce closed-mode binuclear complexes such as **1a**, we have found that rotations about the central methylene group are facile and can produce open-mode complexes such as **1b** and **1c**, as well as a number of intermediate rotational conformations.

The first structurally characterized eHTP complex was $Co_2(CO)_4(eHTP)^{2+}$ (**2**), which was prepared from the reaction of 2

(1) (a) Washington University. (b) Louisiana State University.

0020-1669/90/1329-3363$02.50/0

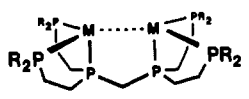

1a

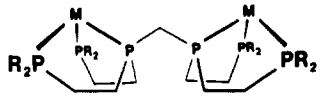

1b

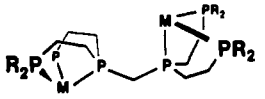

1c

equiv of $CoCl_2$ with eHTP, producing the bimetallic cobalt(II) chloride species, $Co_2Cl_{4-x}(eHTP)^{x+}$ ($x = 0, 2$), followed by reaction with H_2/CO to quantitatively yield **2**.[2] The crystal structure of **2** revealed the open-mode configuration **1b** with a Co–Co separation of 6.697 (1) Å.

This inverted, W-shaped geometry for a bis(phosphino)methane-based linkage was, until recently, unprecedented with respect to both its orientation and the rather large P–CH_2–P angle (127.7 (3)°) present. Singleton and co-workers have reported the first example of a transition-metal bimetallic system with a (diphenylphosphino)methane (dppm) ligand that has this inverted P–CH_2–P orientation, namely, $[\{(\eta^5\text{-}C_5H_5)Ru(1,10\text{-phen})\}_2(\mu\text{-dppm})]^{2+}$, which has the remarkable P–CH_2–P angle of 133.1 (3)°.[3] Because of the ability of eHTP to form this type of conformer, we will make use of the syn and anti nomenclature, commonly applied to pentadienyl systems, to indicate the orientation of the metal atoms with respect to the hydrogen atoms on the bridging methylene group. Syn–syn will, therefore, refer to the rotational conformation **1b** where the metal atoms are on the same side of the methylene group as the hydrogen atoms, likewise, syn–anti for **1c** and anti–anti for **1a**.

The less sterically hindered bis(dimethylphosphino)methane, dmpm, ligand should be able to more readily access the syn–syn mode, but so far this has not been structurally observed. Considering the structure of $[\{(\eta^5\text{-}C_5H_5)Ru(1,10\text{-phen})\}_2(\mu\text{-dppm})]^{2+}$, it should only be a matter of time before more *syn,syn*-bis(phosphino)methane bimetallic systems are crystallographically characterized. One measure of the steric factors involved in the syn–syn orientation, **1b**, for $Co_2(CO)_4(eHTP)^{2+}$ is that the central bridging group has a P–CH_2–P angle of 127.7 (3)°, which can be compared to the 110–118° range normally seen in bis(phosphino)methane bridged dimers.

The four-coordinate, distorted square-planar $M_2Cl_2(eHTP)^{2+}$ (M = Ni, Pd, Pt) complexes provide an interesting example for the flexibility of the central methylene bridge toward bond angle deformations and rotations to give different eHTP configurations. The crystal structure of the BF_4^- salt of $Ni_2Cl_2(eHTP)^{2+}$ reveals a syn–anti conformation similar to **1c**, while the structure of the chloride salt gives an eHTP orientation that is rotated 53° (Ni1–P_{int}··P_{int}–Ni2 torsional angle) from that seen for the BF_4^- salt to give an eHTP rotamer that is about midway between **1b** and **1c**.[4] The palladium and platinum structures, in marked contrast to those seen for the nickel system, adopt a partially closed-mode anti–anti conformation with M–M separations of 4.4217 (8) and 4.6707 (9) Å for Pd and Pt, respectively.[5,6]

Our solid-state structural studies on transition-metal eHTP complexes have probed some of the intriguing questions about the coordination chemistry and intramolecular conformations available to this novel ligand. We now report the rather unusual solvent effects seen in the ^1H NMR spectra of **2** and the spectral assignments based on extensive one- and two-dimensional NMR studies, the results of van der Waals energy calculations on this system, and a qualitative analysis of the conformational dynamics occurring in solution. The reduction chemistry of this complex to produce the closed-mode Co–Co-bonded complex $Co_2(CO)_2$-(eHTP) will also be discussed.

Experimental Section

General Procedures. All manipulations were carried out under inert atmosphere (N_2 or Ar) by using standard Schlenk line or glovebox techniques unless stated otherwise. Solvents were distilled under inert atmosphere from the following drying agents: diethyl ether, hexane, THF (sodium/benzophenone); toluene (sodium); CH_2Cl_2 and acetonitrile (CaH_2); methanol and ethanol (magnesium). eHTP was prepared according to published procedures.[2] ^1H and ^{31}P NMR spectra were run on a Varian XL-300 or VXR-500 spectrometer, IR spectra were run on a Perkin-Elmer 283B or Nicolet 5DXB Fourier transform spectrometer, and NMR simulations were done on a Bruker Aspect 2000 stand-alone data station using the simulation program PANIC.

There is a slow reaction of $Co_2(CO)_4(eHTP)^{2+}$ in most solvents to give a green solution. This is probably caused by gradual diffusion of O_2 into the capped NMR tubes. The formation of a NMR-silent paramagnetic Co(II)–eHTP complex is one likely possibility since the ^1H and ^{31}P NMR spectra of these green solutions appear identical with those of the original yellow samples. The reaction in $CHCl_3$ is much faster than in any of the other solvents and probably implies a direct chlorination type reaction with the solvent itself.

General NMR Spectroscopy. The spectral assignment and conformation of **2** was established through the use of (a) ^1H *J*-resolved spectroscopy with and without ^{31}P decoupling, (b) ^{31}P–^{31}P COSY, and (c) ^1H–^{13}C heteronuclear correlation spectroscopy experiments. *J*-resolved and COSY experiments carried out on the Varian XL-300 spectrometer (^1H resonance frequency at 299.4 MHz) were recorded on approximately 30 mg of **2** in either 0.6 mL of dichloromethane-d_2, methanol-d_4, or dimethyl-d_6 sulfoxide (Merck Sharp and Dome, Rahway, NJ). The ^1H–^{13}C shift-correlated studies were done on a sample containing 60 mg of sample. Experiments carried out on the Varian VXR-500 spectrometer (^1H resonance frequency at 499.6 MHz) were recorded on 10 mg of **2** in 0.7 mL of the appropriate "100%" deuterated solvent (Merck). All simple 1-D spectra were recorded by averaging multiple transients using 45° pulses (XL-300: ^1H, 9 μs; ^{31}P, 18 μs; ^{13}C, 9 μs. VXR-500: ^1H, 4 μs; ^{31}P, 6 μs; ^{13}C, 8 μs). Details on the 2-D experiments are included in supplementary material.

SYBYL **van der Waals Energy Calculations.** The non-hydrogen atom crystallographic coordinates of **2** were entered into the SYBYL program set (version 5.2) and the terminal ethyl groups replaced by methyl groups. Dummy atom types were used for the cobalt metal centers. The use of dummy atoms, which do *not* have van der Waals (VDW) radii associated with them, for the cobalt centers does not adversely affect the VDW calculation, since the steric factors governing the rotational conformers reside completely within ligand–ligand intramolecular contacts. Idealized hydrogen atom positions were calculated by SYBYL and added to the molecule. The two central phosphorus methylene bonds were selected for rotation, and the initial VDW screening factors were set at 50% of their default values. VDW energies (no electrostatic effects were included) were calculated by using the SEARCH routine for 5° rotational increments, and a two-dimensional contour map of the results was generated.

Synthesis of $Co_2(CO)_2$(eHTP) (3). Naphthalene (0.180 g, 1.41 mmol) was weighed into a 300-mL Schlenk flask, and excess sodium-potassium alloy was added. To this was added 200 mL of freshly distilled THF, which immediately took on the characteristic green color of the naphthalenide radical anion. This was stirred for 2 h, and then the stirring was stopped and the solution allowed to settle for 30 min. This dark green solution was added dropwise to a solution of yellow $[Co_2(CO)_4(eHTP)^{2+}][PF_6^-]_2$[1] (0.750 g, 0.705 mmol) in 400 mL of THF over 2.5 h. The reaction solution darkened steadily from its initial light yellow to a dark brown at the end of the addition. Care was exercised to not let any of the excess Na/K alloy transfer over to the reaction flask. The solvent was removed by vacuum evaporation and the resulting solid washed several times with hexane to remove naphthalene. The remaining brown solid was washed with four 25-mL portions of toluene, and the mixture was filtered through Celite to give a clear dark brown solution. This was concentrated to yield a dark brown solid. The solid and solutions of the solid are very sensitive to O_2. Attempts to chromatograph solutions on a variety of supports (silica, alumina, Florisil) caused the decomposition of the spectroscopically identified $Co_2(CO)_2$(eHTP) species. The similar solubility of the various other products present also prevented selective recrystallization. On the basis of the integration of the ^{31}P NMR spectrum of this mixture, $Co_2(CO)_2$(eHTP) accounts for roughly 40–50% of the product. $^{31}P\{^1H\}$ NMR (C_6D_6, δ, H_3PO_4 refer-

(2) Askham, F. R.; Stanley, G. G.; Marques, E. C. *J. Am. Chem. Soc.* **1985**, *107*, 7423.
(3) Albers, M. O.; Liles, D. C.; Robinson, D. J.; Singleton, E. *Organometallics* **1987**, *6*, 2179.
(4) Laneman, S. A.; Stanley, G. G. *Inorg. Chem.* **1987**, *26*, 1177.
(5) Saum, S. E.; Stanley, G. G. *Polyhedron* **1987**, *6*, 1803.
(6) Saum, S. E.; Laneman, S. A.; Stanley, G. G. *Inorg. Chem.*, in press.

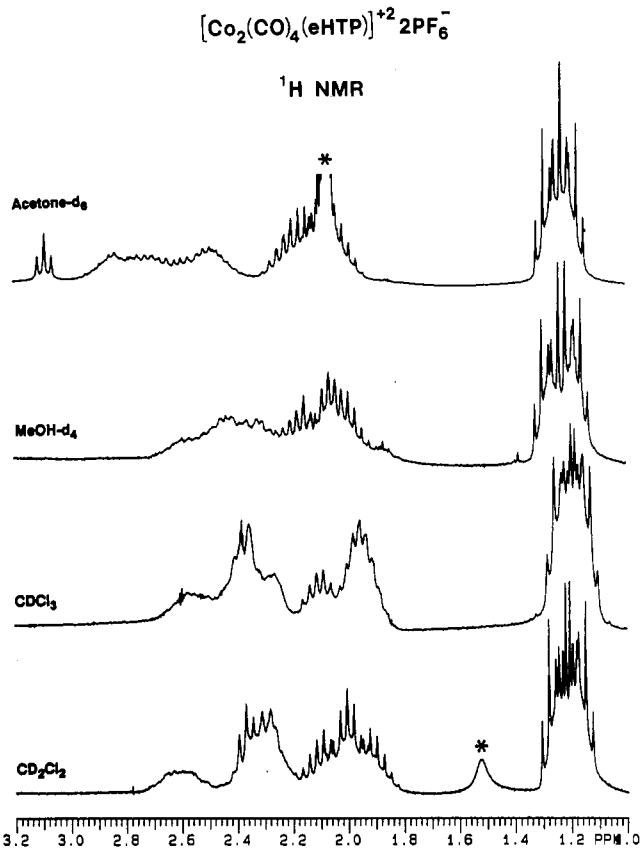

Figure 1. 300-MHz ^1H NMR spectra of $Co_2(CO)_4(eHTP)^{2+}$ (**2**) in the deuterated solvents shown. The starred and truncated peak in acetone is from the solvent, while the starred peak in CD_2Cl_2 is from H_2O, which is present as a solvent of crystallization in samples of **2**.

ence) of $Co_2(CO)_2(eHTP)$ (ppm): 79.8 (m, 4 P) and 103.7 (m, 2 P). ^{31}P coupling constants (absolute values) based on an $A_2XX'A_2'$ simulation (Hz): 51 (P_{int}–P_{int}) and 47 (P_{ext}–P_{int}). The IR spectrum of the product mixture (KBr) showed ν_{CO} peaks at 2010 (s), 1955 (sh), 1927 (vs), 1908 (sh), and 1830 cm^{-1} (vs), as well as peaks characteristic of eHTP.

Results and Discussion

NMR Studies. The presence of ^{31}P nuclei in chemical systems often complicates ^1H NMR studies because of extensive ^{31}P–^1H as well as ^1H–^1H couplings. This is a common problem in many inorganic or organometallic systems where phosphine ligands are routinely employed. An example of this is shown in the 300-MHz ^1H NMR spectra for $[Co_2(CO)_4(eHTP)^{2+}][PF_6^-]_2$ (**2**) in various solvents, which are presented in Figure 1. This molecule not only exhibits complex spectra from extensive ^{31}P and ^1H couplings but also shows significant solvent-dependent changes in both the patterns and chemical shifts of resonances in the region of 1.8–3.2 ppm. Perhaps the most obvious difference in the various spectra shown in Figure 1 is the well-resolved triplet at 3.1 ppm in acetone-d_6, which appears to be absent in the other solvents. In order to deconvolute and thus better understand the solution-state structure of this molecule, we have taken advantage of ^{31}P decoupling in conjunction with two-dimensional NMR methods. Routine ^{31}P decoupling experiments similar to those reported here may prove very useful in simplifying highly coupled inorganic or organometallic chemical systems.

The two-dimensional technique that proved to be most useful for our system was the ^1H homonuclear J-correlated experiment,[7] which allows the separation of proton–proton coupling constants from heteronuclear–proton couplings, in this case ^1H–^{31}P coupling. The two-dimensional ^1H J-correlated spectrum (no ^{31}P decoupling) for **2** in acetone-d_6 is shown in Figure 2 (CD_2Cl_2 spectrum is included in supplementary material). The full spectrum of the

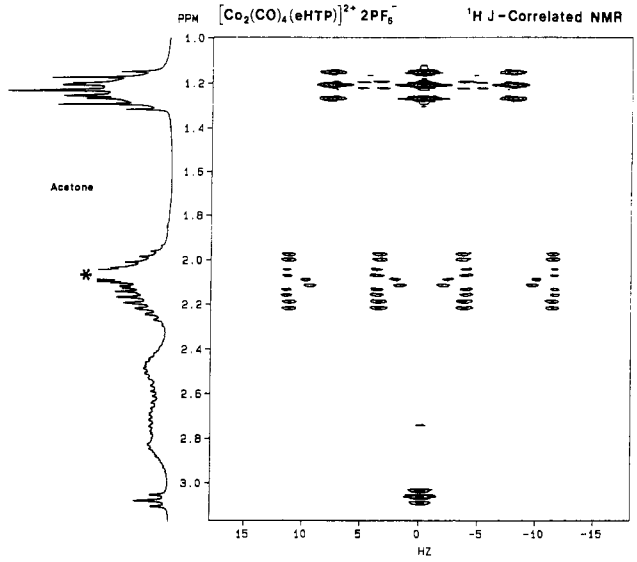

Figure 2. 300-MHz two-dimensional ^1H–^1H J-correlated spectrum of **2** in acetone-d_6 with the corresponding 1-D ^1H spectrum plotted along the vertical ppm axis. The horizontal axis is the ^1H–^1H coupling constant in hertz. The starred, truncated peak in the 1-D spectrum is due to acetone.

acetone-d_6 sample clearly shows features at 1.2, 2.1, and 3.1 ppm, but the region between 2.4 and 2.9 ppm is not resolved, even at lower contour threshold levels. In this ^1H J-resolved experiment a projection onto the chemical shift axis yields the proton-decoupled spectrum, while the ^1H–^1H coupling pattern and constants for each proton are spread out on the horizontal axis, which indicates the coupling constant values in hertz. In Figure 2 we have also plotted the one-dimensional proton-*coupled* spectrum on the vertical axis.

The group of peaks located at 1.2 ppm in both acetone-d_6 and methylene-d_2 chloride appear at first to be three triplets (horizontal pattern) but on closer inspection turn out to be a set of four triplets (J_{H-H} = 7.6 Hz), with two of the triplets overlapping in the center. These correspond to the terminal ethyl CH_3 group protons, which are split into a triplet pattern by the adjacent CH_2 protons. Since the complex probably has C_{2v} symmetry in solution (there is approximate C_{2v} symmetry in the solid state), there should, therefore, only be two unique methyl groups and, hence, *two* triplets in the NMR spectrum. The presence of four triplets might indicate a lowering of the symmetry of the complex, two slightly different species in solution, or the presence of three-bond ^1H–^{31}P coupling, which would split the two expected triplets into a set of four triplets. Any heteronuclear couplings (e.g., ^{31}P–^1H) are, however, also expected to show up as a splitting along the vertical ppm axis. The ^{31}P decoupling experiment offers a straightforward method to clearly differentiate among these possibilities. Our molecule of study, **2**, contains four external and two internal phosphorus atoms whose ^{31}P resonances are separated by 44 ppm. When the external phosphorus atoms were decoupled, the overlapping pattern of four triplets shown in Figure 2 collapsed to only two triplets, conclusively proving that there are only *two* unique ethyl groups in the molecule, confirming our initial assignment of C_{2v} symmetry in solution. One can now readily identify the magnitude of the three-bond H–P coupling constant by measuring the horizontal separation between the triplets to give a sizable $^3J_{H-P}$ of 14 Hz.

The next region of the spectrum examined was the overlapping but well-resolved pattern around 2.1 ppm. Two-dimensional J-correlated spectroscopy allows one to almost completely deconvolute this overlapping set of peaks and, in the case of the acetone-d_6 system, to substantially suppress the solvent peak (see Figure 2) by taking advantage of its longer T_1. This region is now seen to be composed of eight quartets with some interleaved doublet–doublet resonances. The quartets represent the CH_2 protons on the terminal ethyl groups, and the proton–proton coupling involves the three adjacent, equivalent CH_3 hydrogen

(7) Bax, A. *Two Dimensional Nuclear Magnetic Resonance in Liquids*; Delft University Press and D. Reidel Publishing Co.: Boston, MA, 1984.

atoms. Although there are only two unique ethyl groups in the complex, the CH_2 hydrogen atoms on each ethyl group are diastereotopic. We, therefore, expect to see four sets of signals for the four different CH_2 protons. The observation of simple quartets (J_{H-H} = 7.6 Hz) indicates that little or no geminal coupling is present between these hydrogen atoms. Finally, since there should be an observable two-bond $H-P_{ext}$ coupling, the four quartets should be split vertically into eight quartets, or four pairs of quartets, which is exactly what we observe. The spectrum in the CD_2Cl_2 solvent system also clearly shows the four pairs of quartets with the same $^2J_{H-P}$ coupling of 8 Hz.

Selective ^{31}P decoupling of the external phosphorus atoms during the *J*-correlated experiment also confirms our assignment, as the eight quartets collapse down to four quartet resonances. Decoupling the internal phosphorus atoms, moreover, has no effect on this region of the spectrum. The coupling of the ethyl group CH_2 hydrogen atom quartets at 2.1 ppm with the CH_3 hydrogen triplets at 1.2 ppm was further confirmed by a standard $^1H-^1H$ COSY experiment, which showed the expected cross peaks between these two regions. We will return later to discuss the nature of the doublet–doublet resonance that is interleaved in the quartet region.

The feature that attracted most of our initial attention, however, was the well-resolved triplet at 3.1 ppm in acetone, but which appeared to be missing in most of the other solvents. The preliminary assumption that this triplet was due to the central methylene bridge was confirmed by ^{31}P decoupling in conjunction with either one- or two-dimensional experiments. Figure 2 shows that the 2-D *J*-correlated pattern for this resonance at 3.1 ppm is a *vertical* triplet, which shows that the coupling causing the triplet is from two phosphorus centers and *not* from other hydrogen atoms. This immediately narrows the assignment to the central $P-CH_2-P$ methylene group, with the ^{31}P-decoupled one- and two-dimensional spectra demonstrating that irradiation of the internal phosphorus atoms produces a singlet for this resonance, conclusively showing that coupling is only to the internal phosphorus atoms. The position of the bridging methylene signal in CD_2Cl_2 solvent was found in the *J*-correlated ^1H spectrum (figure in supplementary material) at 2.4 ppm, a shift of 0.7 ppm upfield from the same resonance in acetone-d_6. The J_{H-P} coupling constant of 8 Hz is the same as that seen in acetone.

The last portion of the NMR spectrum of **2** that we will examine is the region due to the hydrogen atoms on the ethylene groups that are part of the five-membered chelate rings. All four protons on this ethylene moiety should be different and are expected to exhibit both $^1H-^1H$ and $^1H-^{31}P_{int,ext}$ couplings. Also, if C_{2v} symmetry is present, each chelate ring should be related to one another, giving rise to a single set of four ^1H resonances. Since we have already assigned the three prominent features for **2** in acetone-d_6 (Figure 2) at 1.2, 2.1, and 3.1 ppm as the CH_3 and CH_2 portions of the terminal ethyl groups and the central bridging methylene, the remaining features between 2.1 and 3.0 ppm should be due to the chelate ring protons. Unfortunately, as Figure 2 indicates, the resonances in the 2-D *J*-correlated spectrum for this region are not observed. Using a lower contour threshold shows resonances barely above the noise level beginning to be resolved. Observation of these resonances is hampered by both their rapid relaxation rates and by extensive coupling. This is because relaxation, rapid or on the same time scale as t_1 (evolution period), diminishes the information encoded in the t_2 domain. This problem is further complicated by additional refocusing delays in the heteronuclear correlated experiment. The net result is that short-lived coherences are not able to encode information to the free induction decay, so information about them is lost.

We are able to lengthen the relaxation times of all proton resonances by carrying out our experiments at 40 °C instead of room temperature. The bridging methylene protons show an increase in T_1 from 150 to 350 ms in going to 40 °C where the samples are stable over the time period of the experiment. Selective ^{31}P decoupling also helped to minimize the signal dispersion problem in this region. The last enhancement was to weight the earlier part of the FID more heavily so as to favor the short T_1 signals. In spite of all these enhancement techniques only a small improvement in the resolution of this region was observed at 300 MHz.

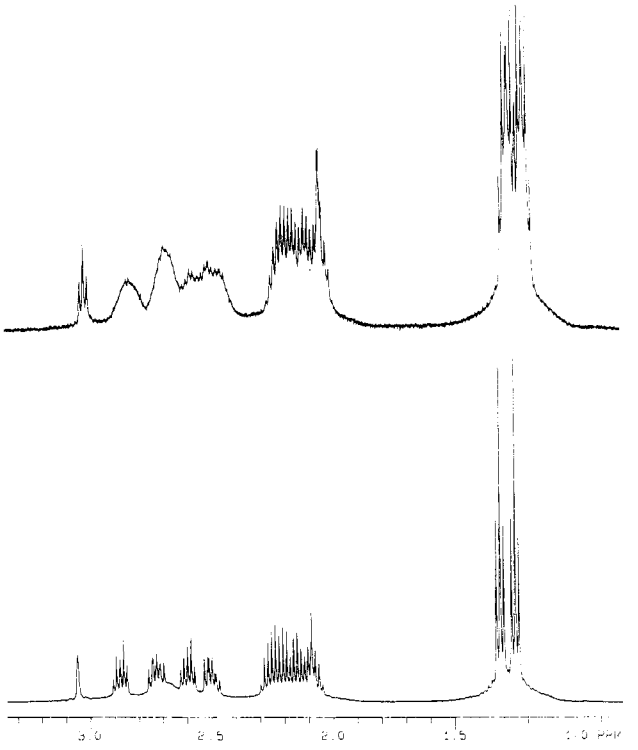

Figure 3. (a) Top: 500-MHz ^1H spectrum of **2** in acetone-d_6. (b) Bottom: 500-MHz broad-band ^{31}P-decoupled ^1H spectrum.

The ^1H spectra of **2** show that the chelate ring resonances retain their complexity even at 500 MHz (see Figure 3a). On the 500-MHz spectrometer, however, we could implement *broad-band* ^{31}P decoupling, which caused a spectacular enhancement of this ill-resolved region, as can be seen in Figure 3b. The four different chelate ring proton resonances are now clearly resolved, and although they appear to be higher order patterns (we have observed field-dependent shifts in these resonances that indicate non-first-order behavior), they can be approximately treated as triplets of doublets. This is qualitatively what one would expect from the one geminal and two vicinal $^1H-^1H$ couplings with two of these coupling constants being approximately equal. The 2-D $^1H-^1H-\{^{31}P\}$ *J*-correlated spectrum (figure included in supplementary material) now clearly resolves these resonances. One explanation for the complexity of this region in the non-^{31}P-decoupled spectrum is that $^1H-^{31}P$ couplings to both P_{int} and P_{ext} are present for these chelate ring resonances. We did not, however, see such a dramatic resolution of the chelate ring resonances in the 500-HMz $^1H\{^{31}P\}$ spectrum in CD_2Cl_2. There is some sharpening of the resonances but nothing like that seen for the acetone-d_6 spectrum. We believe that the reason for this is tied into overlapping chelate ring resonances (vide infra).

The 300-MHz 1-D $^{13}C\{^1H\}$ spectrum of **2** in CD_2Cl_2 has resonances at 8.2 (s, $-PCH_2\mathit{C}H_3$), 22.8 and 23.9 (t, $-\mathit{C}H_2CH_3$, J_{P-C} = 13.5 Hz), 27.0 (dt, $P_{int}-CH_2\mathit{C}H_2-P_{ext}$, J_{P-C} = 12.0 and 15.7 Hz), 29.8 (m, $P_{int}-\mathit{C}H_2CH_2-P_{ext}$), and 31.9 ppm (s, $P-\mathit{C}H_2-P$). The two different methyl group ^{13}C resonances are coincidently degenerate at 8.2 ppm, while the triplets observed for the $-P\mathit{C}H_2CH_3$ carbons arise due to virtual coupling between the two semitransoidal external phosphorus groups. Interestingly, only a singlet is observed for the central methylene carbon atom despite it being directly bound to two phosphorus atoms. These assignments were verified by performing $^1H-^{13}C$-correlated experiments on **2** in CD_2Cl_2. Sensitivity was a problem, however, since the cross-peaks in the resulting spectrum are split in both dimensions by ^{31}P coupling to the ^1H and ^{13}C nuclei. This is at its worst for the chelate ring $^1H-^{13}C$ correlations. The short T_1's for the chelate

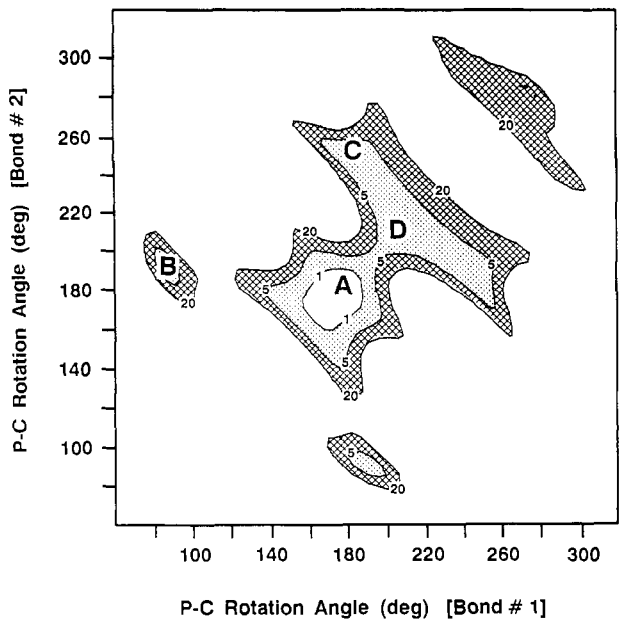

Figure 4. van der Waals (VDW) energy map for a model complex of **2** derived from the crystallographic coordinates of the PF_6^- salt structure.[2] The axes represent rotations in degrees about the two central P–CH_2–P bonds with the contour values showing the relative VDW energy in kcal/mol up to a maximum of 20 kcal/mol. This energy map is approximately symmetric about the diagonal. The location of the global minimum is shown by the label A, which is nearly coincident with the rotational conformation observed for the crystal structure. Other local minima in increasing energy are labeled B–D.

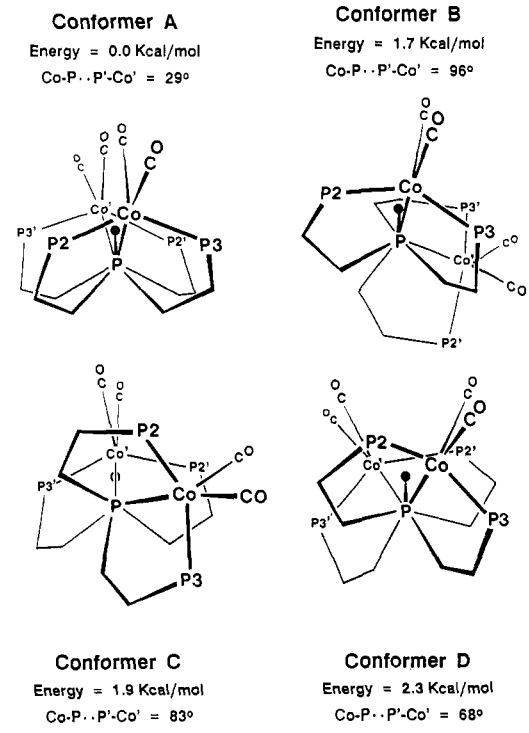

Figure 5. Simplified stick diagram representations for conformers A–D from the VDW energy calculation. Terminal methyl groups and hydrogen atoms have been omitted for clarity, and the view shown is projected down the central P_{int}··P_{int} axis to highlight the rotational conformation (only one of the internal phosphorus atoms is shown). The central methylene bridge is oriented up in each view and highlighted by a heavy dot for reference. The relative VDW energies and Co–P_{int}··P_{int}–Co′ torsional angles are listed for each conformer. Conformer A is essentially the same as observed in the crystal structure of **2**.

ring protons likely are responsible for the degradation of these cross-peaks. Unfortunately, we did not have a three-channel probe, which would allow us to implement ^{31}P decoupling during the ^1H–^{13}C correlation experiment. The 2-D ^1H–^{31}P hetcor experiment that was attempted early on to verify the nature of the methylene bridge triplet resonance also suffered severely from the short T_2's of the phosphorus resonances. We attribute the short ^{31}P T_2 times to the directly bound quadrupolar cobalt atoms, which provide an efficient relaxation pathway (scalar relaxation of the second kind).

The one feature in the ^1H spectrum that we have neither assigned nor understand is the doublet–doublet pattern in the middle of the $-PCH_2CH_3$ quartets at 2.15 ppm in Figure 2. A similar feature is also observed in the CD_2Cl_2 solvent system. In the acetone-d_6 spectrum this doublet–doublet resonance is very temperature dependent with the larger coupling constant at 300 MHz varying from 8.4 Hz (52 °C) to 23.2 Hz (−39 °C), while at 500 MHz the larger coupling constant ranges from 22 Hz at 45 °C to approximately 46 Hz at −45 °C. The marked field dependence for this resonance points to a non-first-order pattern, which, in turn, implies that the resonance is not a simple doublet–doublet. We initially suspected that this resonance was due to some impurity or the result of some decomposition, but this possibility was investigated by using a freshly prepared solution of high-purity 100% acetone-d_6 and a doubly recrystallized sample of **2** with this resonance still being observed. There is ^{31}P coupling to this resonance which disappears on phosphorus decoupling implying that it is connected in some way to eHTP, but we have not developed any satisfactory explanation for its origin.

van der Waals Energy Calculations. In order to more fully probe the rotational flexibility about the central methylene bridge, we performed van der Waals (VDW) energy calculations on the various rotamers by using the SYBYL molecular mechanics/graphics program set.[8] This very simple type of steric energy calculation has proven to be quite valuable in enabling us to understand conformational preferences in our nickel and group VI bimetallic systems even with the restraints of using a rigid, simplified model complex.[4,6,9] The results of the VDW energy calculation are summarized in Figure 4, which shows an expanded portion of the two-dimensional energy map. The two axes represent the angle of rotation about the two central phosphorus–methylene group bonds, while the contours indicate the relative VDW energies in 1, 5, and 20 kcal/mol increments. The map is approximately symmetrical about the diagonal because of the crystallographic 2-fold symmetry of the starting $Co_2(CO)_4$(eHTP)$^{2+}$ molecule used. Exact symmetry is not seen because the two five-membered chelate rings on the unique half of **2** have slightly different ring puckerings that cause different VDW atom–atom contacts. In solution, of course, one would expect these slight differences to average out to give a fully symmetrical map. The origin of the map (0°, 0° or 360°, 360°) corresponds to the closed-mode conformation **1a**.

It is important to note that the energy evaluation scheme used in the VDW calculation tends to *over*estimate atom–atom contact energies, so although the regions of low energy are certainly qualitatively correct, other higher energy regions and especially barrier heights may be actually quite a bit lower in energy than indicated.[10] Because of the rigid model being used and the simplicity of the VDW calculation, we estimate that for the low-energy regions values within ca. 2 kcal/mol should be considered approximately equivalent. In spite of this, we will continue to report energy values typically to one decimal place.

The global minimum for the VDW energy calculation is located at the position labeled A on the map in Figure 4, whose energy has been set to 0.0 kcal/mol. The observed crystal structure conformation is only 10° away from the global minimum and can

(8) (a) Naruto, S.; Motoc, I.; Marshall, G. R.; Daniels, S. B.; Sofia, M. J.; Katzenellenbogen, J. A. *J. Am. Chem. Soc.* **1985**, *107*, 5262. (b) The SYBYL program set is available from TRIPOS Associates, Inc., 1699 S. Hanley Rd., Suite 303, St. Louis, MO 63144.

(9) Saum, S. E.; Askham, F. R.; Fronczek, F. R.; Stanley, G. G. *Organometallics* **1988**, *7*, 1409.

(10) Richards, A. (Tripos Associates), Tripos Users Meeting, St. Louis, MO, June, 1987.

be considered isoenergetic with an energy of 0.1 kcal/mol. There are several other low-energy local minima on the map: the position labeled B has a VDW energy of 1.7 kcal/mol, while the position labeled C has an energy of 1.9 kcal/mol. Regions B and C have symmetry-related minima on the other side of the map diagonal that are not labeled to keep the map from getting too cluttered. The position labeled D is a shallow local minimum with an energy of 2.3 kcal/mol. Stick diagrams of conformers A–D are shown in Figure 5, viewed down the central P_{int}–P_{int} vector to highlight the rotational differences between the various conformations. The bridging central methylene group in each case is oriented up and is emphasized by a heavy dot for reference. The Co–P_{int}··P_{int}–Co′ torsional angles for each conformer are also listed in Figure 5.

Another important piece of information that these VDW calculations give is an upper estimate of the barriers for rotations from one minimum to another. The barrier for rotation from A to D, for example, is only 4.3 kcal/mol, while there is essentially no barrier for rotations from D to C. The barrier from region A to B is a more substantial 33 kcal/mol, but even this is probably overestimated to some extent with the result that rotations between B ⇄ A ⇄ D ⇄ C are most likely all thermally accessible. It is clear, however, that conformers A, D, and C belong to a particularly large and low-energy region and that rotations between these conformers should be especially facile. This can be probed to a certain extent by relaxing the relatively large central methylene bridge angle of 127.6° and recalculating the VDW energy map. Reducing the P–CH_2–P angle to 123, 120, and finally 117° causes the low-energy region encompassing conformers A, C, and D to gradually shrink in size. Region B, however, recedes much more rapidly and essentially has disappeared (i.e, has an energy greater than 20 kcal/mol higher than that for A) at a methylene bridge angle of 117°, while there is still a well-defined global minimum in the same area as A and a local minimum at D. The barrier between A and D at 117° is 75 kcal/mol, but it is quite likely that this is overestimated.

Conformational Dynamics. It seemed a reasonable proposition that the rotational conformation of eHTP about the central methylene bridge and variations in the P–CH_2–P bond angle should have an effect on the position of the ^{1}H NMR resonance for this group. Furthermore, there appears to be a dynamic process occurring for **2** in acetone-d_6 on the basis of the low-temperature ^{1}H NMR spectrum. Figure 6 shows the 500-MHz ^{31}P-decoupled variable-temperature proton spectra between +45 and −45 °C for an expanded region of **2** in acetone-d_6. Once again, the most dramatic feature of the spectrum is the downfield shifting of the resonance due to the bridging methylene protons. We have examined the variable-temperature spectra in acetone, CD_2Cl_2, and acetonitrile with only acetone-d_6 showing any significant temperature-dependent effects.

We propose that the variability of the chemical shift of the P–CH_2–P resonance is related to the rotational flexibility of the bis(phosphino)methane bridge and the shielding properties of the carbonyl ligands. The shielding effects of metal-bound carbonyls have been explored, and both distance and orientation of the carbonyl with respect to the observed nucleus were shown to be important in determining the sign and magnitude of the shielding interaction.[11] The crystal structure of **2** indicates that the bridging methylene group hydrogen atoms are quite exposed to the inward-pointing carbonyl π systems. Rotation about the central carbon–phosphorus bonds changes both the distance and mutual orientations of the hydrogen atoms and carbonyl ligands, thereby perturbing the shielding value.

One can easily measure approximate CO··H_2C contact distances (values reported are the OC··H distances) for the various conformers calculated in the VDW energy calculation. Conformer A, which corresponds to the crystal structure, has a minimum CO··H_2C separation of 3.0 Å, while for conformer D this distance shortens to a remarkably close 2.5 Å. Conformers B and C also have short CO··H_2C contacts around 2.6 Å. One would expect

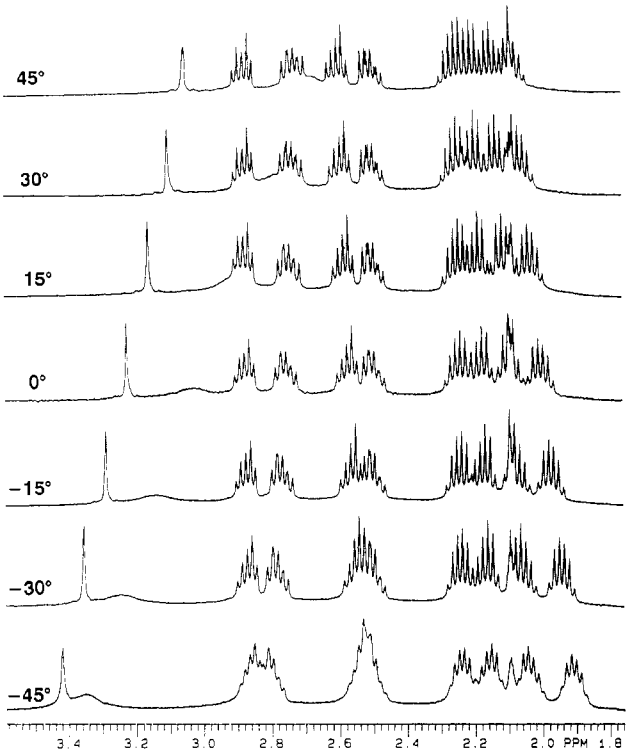

Figure 6. Variable-temperature 500-MHz ^{1}H{^{31}P} spectra for **2** in acetone-d_6. The small, barely observable broad resonance that moves rapidly downfield with decreasing temperature is due to H_2O present in **2** as a solvent of crystallization.

the presence of conformers B, C, and/or D to cause an enhanced shielding and upfield shifting of the central methylene resonance.

The presence of different rotational conformers nicely explains the changes in the central methylene resonance in different solvents and agrees well with our previous work on the solid-state vs solution conformations for $M_2(CO)_6$(eHTP) (M = Cr, Mo, W).[9] The movement of this resonance in the variable-temperature spectra in acetone-d_6 can be explained by a fast dynamic equilibrium between conformers A and C that gives rise to a single averaged resonance for the P–CH_2–P protons. The decrease in temperature causes a change in the relative amounts of each conformer present with lower temperatures giving rise to a downfield shift for this resonance. Since the carbonyl shielding effect decreases with distance, A is implicated as the lower energy conformer in acetone-d_6. This is in accord with the results of the VDW energy calculations discussed earlier.

In other solvents such as CD_2Cl_2 where no temperature-dependent shifts in the position of the central methylene bridge protons are observed, one of the associated rotational conformers is now stable enough to result in a static or dominant solution structure. The presence of a simple triplet for the P–CH_2–P ^{1}H resonance in CD_2Cl_2 indicates that the averaged solution structure gives rise to a symmetrical environment about the methylene bridge.

This corresponds nicely to the calculated conformer D, which is symmetrically splayed about the central methylene bridge. A static conformer such as C would give rise to an asymmetric environment, and one would expect to see two resonances for the central methylene bridge protons that should have a doublet of triplets, or pseudoquartet pattern. Conformation C is possible if there is a fast rotation between the two diagonally related positions (one is not labeled) on the VDW map in Figure 4 in which conformer D is at the midpoint in this rotation. This would give rise to an averaged symmetric structure that would have a considerable amount of carbonyl shielding and a simple triplet pattern for the central methylene protons.

Another possibility for solvents such as CD_2Cl_2 where no temperature-dependent shifts in the position of the central methylene bridge proton resonances are observed is that con-

(11) McGlinchey, M. J.; Burns, R. C.; Hofer, R.; Top, S.; Jaouen, G. *Organometallics* **1986**, *5*, 104.

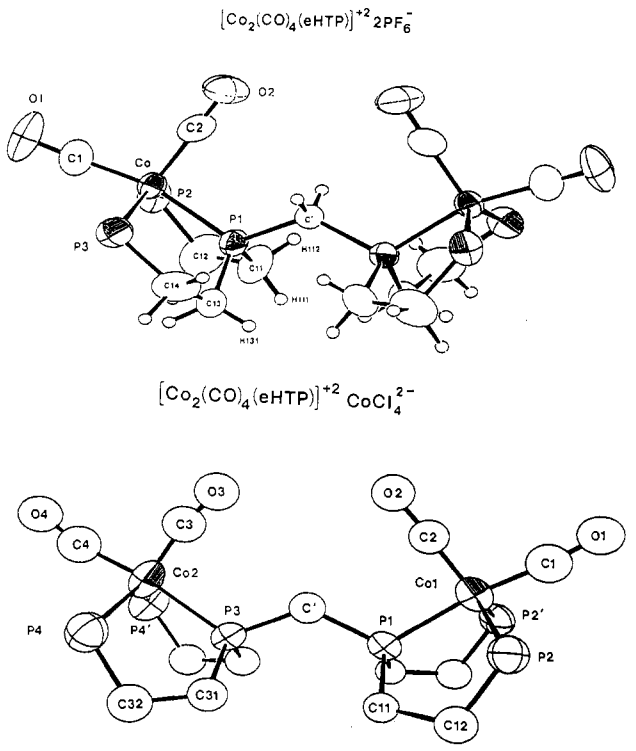

Figure 7. ORTEP plots of the X-ray structures of the $Co_2(CO)_4(eHTP)^{2+}$ portion for the PF_6^- (top) and $CoCl_4^{2-}$ (bottom) salts.[2]

formers A and C/D are isoenergetic. In this case temperature changes will not perturb the equilibrium populations of the conformers. We do not favor this explanation, however, because conformers A and C would each have to be present in equal concentrations and the P–CH_2–P proton resonances would occur at their averaged chemical shift positions. The most downfield position of the methylene bridge ^1H resonance in acetone-d_6 that we have observed is at 3.42 ppm (−45 °C). The location of this same resonance in CD_2Cl_2 is at 2.37 ppm. If one assumes that this is the average position, then the location of this resonance for the other conformer would be 1.32 ppm. We feel that this value is too low considering the amount of carbonyl shielding possible relative to reasonable CO··H_2C contact distances.

Careful examination of the chelate ring proton resonances in the various solvents reveals that there are chemical shift differences for these as well. We propose that changes in these resonances are tied into trigonal-bipyramidal (TBP) and square-pyramidal (SP) geometry changes about the cobalt centers. The energetic availability of both TBP and SP geometries for **2** is clearly demonstrated by the crystal structures on the PF_6^- and $CoCl_4^{2-}$ salts of **2** shown in Figure 7. The PF_6^- salt of $Co_2(CO)_4(eHTP)^{2+}$ has a distorted SP coordination geometry about each cobalt center with a P2–Co–P3 angle of 135°, while the $CoCl_4^{2-}$ salt has a nearly ideal TBP environment.[2] The structure of the $CoCl_4^{2-}$ salt of **2** was only briefly mentioned in the experimental section of ref 2 due to a poor-quality data set caused by the small size of the crystals obtained and a partial occupancy problem. The $Co_2(CO)_4(eHTP)^{2+}$ cation lies on a mirror plane that passes through the two cobalt atoms, the carbonyl groups, and the central methylene bridge. The complex is, therefore, completely eclipsed. The fact that crystal packing forces can cause a change in coordination geometry about the metal centers implies a relatively small energy difference between these two configurations. One would, therefore, expect that solution effects could also access both TBP and SP geometries. Note that the chelate ring puckerings in the two structures (Figure 7) are quite different: the TBP $CoCl_4^{2-}$ salt has chelate ring orientations that are "tucked in", while the SP PF_6^- salt chelate rings are splayed outward. These different ring puckerings should affect the chemical shift environments of the chelate ring proton resonances. We, therefore, believe that the changes in the chemical shift positions of the chelate ring protons are tied into TBP ⇄ SP interconversions on the cobalt atoms.

The 1-D ^1H NMR spectrum of **2** in CD_2Cl_2 (see Figure 1) has the chelate ring resonances concentrated in two unresolved regions at 2.3 and 2.6 ppm. As we have seen for acetone-d_6, there are four well-resolved resonances in the 500-MHz ^{31}P-decoupled ^1H spectra at higher temperatures (see Figure 3) that one can correlate to the same unresolved region in the 300-MHz acetone-d_6 spectrum in Figure 1. We tentatively propose that, in the TBP structure, the tucked in nature of the chelate ring conformation enhances the distinct inner and outer chemical shift environments for the chelate ring hydrogen atoms in addition to the chemical shift variations inherent for the two different methylene groups on the P_{ext}–CH_2CH_2–P_{int} linkage. We tentatively propose that in the TBP structure the tucked in nature of the chelate ring conformation causes a greater chemical shift dispersion for these protons than in the splayed out SP structure. If the solution structure is considered to be in equilibrium between the TBP and SP geometries, then at room temperature the SP geometry is more dominant in CD_2Cl_2 than it is in acetone-d_6. This conclusion is supported by calculation of the OC–Co–CO angle from the intensity ratio of the symmetric and asymmetric carbonyl stretching modes from the IR solution spectra of **2**.[12] In acetone this calculated angle is 92°, while in dichloromethane it has increased to 96°. Although this difference is small, it is in the proper direction and in good agreement with the OC–Co–CO angles observed in the TBP and SP X-ray structures for the $CoCl_4^{2-}$ and PF_6^- salts of **2** of 91 and 99°, respectively.

The variable-temperature 500-MHz $^1H\{^{31}P\}$ spectra in acetone-d_6 (Figure 6) show that as the temperature is lowered, the pattern for the chelate ring resonances in the 2.4–2.9 ppm region change in a manner suggestive of an increase in the importance of the SP geometry. Thus, it appears that the SP geometry is lower in energy than the TBP geometry in both acetone and dichloromethane but that the magnitude of this energy separation is smaller in acetone than in CH_2Cl_2. So, in acetone-d_6 two fast conformation processes are observed: rotation about the central methylene bridge to give differing amounts of carbonyl shielding on the P–CH_2–P ^1H resonances and TBP ⇄ SP coordination geometry interconversions that affect the chelate ring resonances.

Reduction Chemistry. The syn–syn open-mode conformation observed for $Co_2(CO)_4(eHTP)^{2+}$ is the expected conformation on the basis of the fact that the Co(1+) centers have five ligands about them and an 18-electron configuration. Reduction of this complex by two electrons (one electron per cobalt), however, should force the dissociation of one ligand from each metal center, giving rise to four-coordinate 17-electron Co(0) atoms that should want to close up and form a Co–Co bond. We have performed another VDW energy calculation on our model complex of $Co_2(CO)_4(HTP)^{2+}$ with the two internal carbonyl ligands removed. The calculation clearly indicates that for this "reduced" complex the closed-mode geometry, **1a**, is now sterically accessible with an energy of only 4 kcal/mol above the global minimum. Note that the VDW calculation has no information about any potential M–M bonding interactions between the cobalt centers.

One potential problem with the reduction of **2** is that dissociation of either a carbonyl or phosphine ligand can occur.[13] Loss of a phosphine is, of course, inhibited by the chelate effect, while reduction of the cobalt center will increase the Co–CO π backbonding and inhibit the dissociation of the carbonyl ligand. It was not too surprising, therefore, that a number of diamagnetic CO and phosphine-dissociated products result from the reduction of **2** with 2 equiv of naphthalenide anion.

The ^{31}P NMR spectrum of the reaction mixture, however, provides compelling evidence for the formation of a symmetrical Co–Co-bonded closed-mode dimer, $Co_2(CO)_2(eHTP)$ (**3**). The ^{31}P–^{31}P two-dimensional COSY spectrum of the reaction mixture is shown in Figure 8a and allows the unambiguous assignment

(12) Cotton, F. A.; Wilkinson, G. *Advances Inorganic Chemistry*, 4th ed.; Wiley: New York, 1980; pp 1075.
(13) Kuchynka, D. J.; Kochi, J. K. *Inorg. Chem.* **1988**, *27*, 2574.

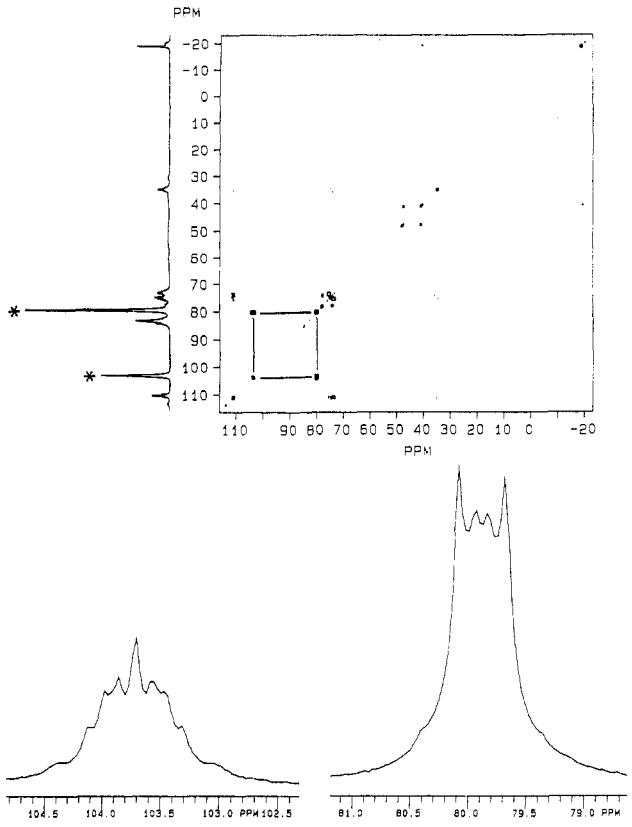

Figure 8. (a) Top: 2-D ^{31}P chemical shift correlated NMR spectrum of the product mixture from reduction of **2** with 2 equiv of naphthalenide anion. The 1-D $^{31}P\{^1H\}$ spectrum is plotted along the vertical axis for reference. (b) Bottom: expansion of the two ^{31}P resonances assigned to $Co_2(CO)_2$(eHTP).

of resonances to the same molecule through their scalar couplings. This spectrum clearly establishes connectivity between the resonances at 79.8 and 103.7 ppm with no other correlations to either of these two peaks. It is also evident from the resonances around −20 ppm in the ^{31}P spectrum that several species with dangling, uncoordinated phosphine ligands have also formed.

An expanded view of the one-dimensional ^{31}P NMR spectrum for the two peaks assigned to **3** is shown in Figure 8b. The presence of only two ^{31}P resonances for this species points directly to a symmetrical dimer with only two phosphine environments. The resonance at 103.7 ppm, having half the intensity of the resonance at 79.8 ppm, is assigned to the two internal phosphorus atoms and is completely consistent with the presence of two five-membered chelate rings that cause a substantial downfield ring shift,[14] analogous to that seen for the starting complex **2**.[2] The non-first-order nature of these peaks assures us that these peaks are *not* due to the one-electron reduction product, which would contain isolated Co(I) and Co(0) atoms, since we would expect the odd-electron Co(0) center to paramagnetically decouple the one half of eHTP from the other.[15] The possibility that the diamagnetism of **3** results from the reduction to Co(1−) can be ruled out for several reasons: the solubility of **3** in nonpolar solvents is consistent with a neutral compound; the addition of 2 extra equiv of reducing agent causes these ^{31}P resonances to disappear consistent with the proposed Co(0) formulation.

Finally, we have successfully simulated the ^{31}P NMR spectrum of **3** using an $A_2XX'A_2'$ spin system, which gives a coupling constant of 47 Hz between the internal and external phosphorus atoms, the same that is observed in the starting material **2**. The coupling between the two internal phosphorus atoms, however, has increased by 46% to a value of 51 Hz. This is completely consistent with the formation of a closed-mode compound in which the coordinated phosphorus lone pairs are aligned parallel and subject to increased coupling.[16]

Isolation and further characterization of this compound was hampered by its very reactive nature and the similarity of its solubility properties to those of the other reaction products present (see Experimental Section). The absence of carbonyl absorption frequencies below 1830 cm^{-1} points to a species with only terminal carbonyls. We, therefore, propose the Co-Co-bonded structure shown as

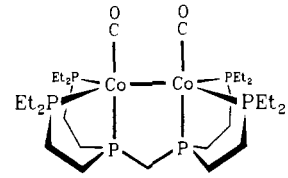

There is only one other analogous cobalt dimer known, $Co_2(CO)_2(PPh_3)_6$, which was isolated in 4% yield upon bubbling carbon monoxide through a THF solution of cobalt(II) stearate, ethylmagnesium bromide, and excess PPh_3.[17]

Summary and Conclusions

The various changes in the ^1H NMR spectra of $Co_2(CO)_4$(eHTP)$^{2+}$ in different solvents and the temperature-dependent behavior in acetone-d_6 have been probed primarily by two-dimensional ^1H–^1H *J*-correlated spectra employing both selective and broad-band ^{31}P decoupling. We have found that the 2-D ^1H–^1H *J*-correlated spectra are extremely useful in deconvoluting complex, overlapping resonances, particularly in systems that possess proton–heteronuclear couplings. The remarkable effect of broad-band ^{31}P decoupling on the ^1H NMR spectra of **2** in acetone provides an elegant example of the importance of this technique in organophosphorus-based systems.

In conjunction with van der Waals energy calculations and solid-state structural studies, two conformational processes have been identified for **2**:

(1) Rotations about the central methylene bridge occur to produce conformers that cause differing amounts of carbonyl shielding on the P–CH_2–P hydrogen resonances. The low-energy conformer, A, similar to that seen in the crystal structure, in which the carbonyl ligands essentially lie in a plane bisecting the central methylene bridge protons results in the minimum shielding effect and the greatest *downfield* shift of the methylene group ^1H resonances. Another set of conformers, C/D, is symmetrically rotated about the P–CH_2–P bonds to generate configurations in which the inward-facing carbonyl ligands are now much closer to the methylene hydrogen atoms causing the maximum amount of shielding and the greatest *upfield* shift of that methylene resonance. In acetone these two conformers have a relatively small energy separation and are in equilibrium; reducing the temperature shifts the equilibrium toward the lower energy conformer A.

(2) The second process that is occurring involves solvent-dependent coordination geometry interconversions about the cobalt centers between trigonal-bipyramidal (TBP) and square-pyramidal (SP) geometries. This geometry change results in chelate ring puckering differences, which, in turn, alters the chemical shift environments for the chelate ring proton resonances. In TBP geometry the two chelate rings on a cobalt center are tucked in toward each other and create an inner and outer set of chelate ring hydrogen atoms maximizing the differences between them. The SP case has the chelate rings splayed outward and apart from one another minimizing the differences between the hydrogen atoms on each carbon atom. Once again we see a dynamic process in acetone where at high temperatures there are four well-resolved chelate ring proton resonances (^{31}P-decoupled 500-MHz spectrum,

(14) Garrou, P. E. *Chem. Rev.* **1981**, *81*, 229.
(15) Askham, F. R.; Saum, S. E.; Stanley, G. G. *Organometallics* **1987**, *6*, 1370.
(16) (a) Keat, R.; Manojlovic-Muir, L.; Muir, K. W.; Rycroft, D. S. *J. Chem. Soc., Dalton Trans.* **1981**, 2192. (b) Colquhoun, I. J.; McFarlane, W. *J. Chem. Soc., Dalton Trans.* **1977**, 1674. (c) Cross, R. J.; Green, T. H.; Keat, R. *J. Chem. Soc., Dalton Trans.* **1976**, 1424.
(17) Simon, A.; Nagy-Magos, Z.; Palagyi, J.; Palyi, G.; Bor, G.; Marko, L. *J. Organomet. Chem.* **1968**, *11*, 634.

Figure 3), which is assigned to an increased contribution from the TBP geometry. As the temperature is lowered, however, the equilibrium shifts to favor the lower energy conformation and the resonances merge into two sets of less well defined resonances that we believe correlate to SP geometry. In solvents such as CH_2Cl_2 and acetonitrile where no temperature-dependent shifts are observed, one conformer has an energy low enough to generate a single dominant SP structure.

The simple VDW energy calculations have, once again, proven to be very useful in helping us qualitatively understand the various rotational conformations possible and the pathway energetics between them. We consider it very important to gain a firm understanding of the rotational dynamics in open-mode bimetallic M_2(eHTP)-type systems so that we can predict when the two metal centers can approach one another to cooperate in the joint activation of a substrate molecule.

The reduction of $Co_2(CO)_4(eHTP)^{2+}$ by naphthalenide anion produces several diamagnetic bimetallic Co(0) complexes involving both carbonyl and phosphine dissociation. On the basis of one- and two-dimensional ^{31}P NMR studies, one of the major products can be confidently assigned as the symmetrical Co–Co-bonded dimer $Co_2(CO)_2$(eHTP), the first example of a M–M-bonded eHTP binuclear species. The very reactive nature of this electron-rich species, unfortunately, kept us from isolating and further characterizing it.

Acknowledgment. This work was supported by the National Science Foundation (Grants CHE-86-13089 and CHE-88-23041). The Washington University High-Resolution NMR Service Facility was funded in part through NIH Biomedical Research Support Shared Instrument Grant 1-S10-RR02004 and a gift from the Monsanto Co. We would also like to thank Dr. Suzanne E. Saum (Washington University) for assistance in preparing a number of NMR samples and Prof. Leslie Butler (LSU) for helpful suggestions.

Supplementary Material Available: Text containing a detailed experimental NMR section and figures of the 300-MHz 2-D ^1H–^1H *J*-correlated spectrum of **2** in CD_2Cl_2 and 500-MHz 2-D ^1H–$^1H\{^{31}P\}$ *J*-correlated spectrum of **2** in acetone-d_6 (5 pages). Ordering information is given on any current masthead page.

Contribution from the Department of Chemistry,
Revelle College, University of California at San Diego, La Jolla, California 92093

Synthesis, Properties, and Structure of Bis(*cis*-(methylthio)stilbenethiolato)nickel(II) and Bis(*cis*-bis(methylthio)stilbene)nickel(II) Iodide

G. N. Schrauzer,* Cheng Zhang, and E. O. Schlemper*,†

Received January 5, 1990

The sulfur atoms in the bis(*cis*-stilbene-1,2-dithiolato)nickel(II) dianion, $[Ni(S_2C_2Ph_2)_2]^{2-}$ = $Ni[S_4C_4Ph_4]^{2-}$, react with alkyl halides to yield unusually stable bis(alkylthio) derivatives of composition $Ni[R_2S_4C_4Ph_4]$, with R = alkyl. The green, diamagnetic complex with R = CH_3 crystallizes in space group $P2_1/n$, with unit cell dimensions at 23 °C of a = 6.127 (3) Å, b = 8.001 (3) Å, c = 27.663 (3) Å, β = 93.81 (2)°, Z = 2, and d_{calcd} = 1.407 g cm^{-3}, and is shown to be bis((methylthio)stilbenethiolato)nickel(II), $Ni[PhC(SCH_3)=C(S)Ph]_2$. The NiS_4 moiety is essentially planar with mean Ni–S bond lengths of 2.161 (2) Å. The observed ligand C–S(CH_3)– and C–S bond lengths of 1.779 (5) and 1.737 (5) Å are in the range of C–S single bonds; the C–C bond distance is 1.352 (7) Å, consistent with an essentially localized electronic structure. The Ni–S–CH_3 bond angles of 105.2 (2)° are smaller than expected due to crystal packing forces. In a 1:1 inclusion compound with CH_2Cl_2, which crystallizes in space group $P\bar{1}$, with unit cell dimensions a = 8.424 (3) Å, b = 13.461 (3) Å, c = 14.745 (3) Å, α = 68.93 (2)°, β = 84.08 (2)°, γ = 75.10 (2)°, Z = 2, d_{calc} = 1.45 g cm^{-3}, the lattice expansion causes a normalization of the Ni–S–CH_3 angles to 109.2 (2)°. Variable-temperature ^1H NMR measurements in solution reveal dynamic equilibria attributed to sulfur inversion and cis–trans isomerization reactions. On heating, decomposition occurs with ligand disproportionation to bis(methylthio)stilbene and nickel(II) stilbenedithiolate, $[Ni(S_2C_2Ph_2)]_x$. The sulfur atoms exhibit residual nucleophilic reactivity on reaction with CH_3I, affording a complex of composition $[(CH_3)_2S_2C_2Ph_2]_2NiI_2$, which crystallizes in space group $P2_1/n$, with a = 8.178 (3) Å, b = 11.992 (3) Å, c = 18.229 (5) Å, β = 94.28 (2)°, Z = 2, d_{calcd} = 1.69 g cm^{-3}. Its structure reveals a linear I–Ni–I moiety with two molecules of symmetrically S-bonded molecules of *cis*-bis(methylthio)stilbene as the ligands in the equatorial positions. The mean Ni–S bond and C–S(CH_3) bond lengths are 2.379 (9) and 1.803 (4) Å, and the mean Ni–I bond lengths are 2.7989 (2) Å, respectively.

Introduction

Complexes of transition metals with substituted or unsubstituted *cis*-ethylene-1,2-dithiols of composition $M(S_2C_2R_2)_2$ = $MS_4C_4R_4$, or $M(S_2C_2R_2)_3$ = $MS_6C_6R_6$, where R may be H, alkyl, aryl, etc., are commonly known[1,2] as metal dithiolenes. After their discovery in 1960,[3,4] they were widely studied because their spectra and chemical properties suggested a high degree of electronic delocalization and the presence of low-lying unoccupied orbitals, rendering them easily reducible to anionic species.

To show that these orbitals were predominantly ligand rather than metal based, as indicated by some of the MO treatments, the dianion $[NiS_4C_4Ph_4]^{2-}$, where Ph = C_6H_5, was reacted with alkylating agents. With methyl iodide a neutral dimethyl derivative of composition $Ni[(CH_3)_2S_4C_4Ph_4]$ (**1**) was obtained, for which structures **1A–C** are possible. Structure **1A** was suggested,[5] as bis(methylthio)stilbene (**2**) was formed on thermolysis or on reaction with 2,2′-bipyridyl (eq 1).

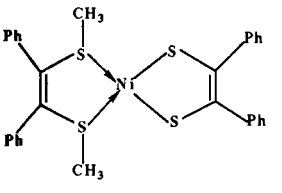

1A

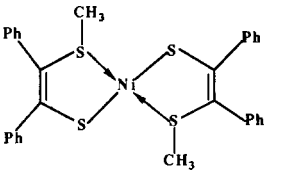

1B

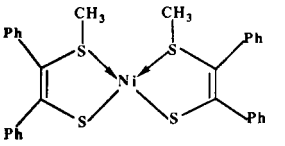

1C

In 1978, Eckstein and co-workers[6] suggested that **1** had structure **1B**, since the disulfide $[CH_3S–C(Ph)=C(Ph)–S]_2$ (**4**)

† Department of Chemistry, The University of Missouri, Columbia, MO 65211.

0020-1669/90/1329-3371$02.50/0